Plasmon resonance in warm dense matter

R. Thiele,* T. Bornath, C. Fortmann, A. Höll, R. Redmer, H. Reinholz, G. Röpke, and A. Wierling
Institut für Physik, Universität Rostock, D-18051 Rostock, Germany

S. H. Glenzer
L-399, Lawrence Livermore National Laboratory, University of California, P.O. Box 808, Livermore, California 94551, USA

G. Gregori
Clarendon Laboratory, University of Oxford, Parks Road, Oxford, OX1 3PU, United Kingdom
and CLF, Rutherford Appleton Laboratory, Chilton, Didcot OX11 0QX, United Kingdom
(Received 29 February 2008; revised manuscript received 23 May 2008; published 21 August 2008)

Collective Thomson scattering with extreme ultraviolet light or x rays is shown to allow for a robust measurement of the free electron density in dense plasmas. Collective excitations like plasmons appear as maxima in the scattering signal. Their frequency position can directly be related to the free electron density. The range of applicability of the standard Gross-Bohm dispersion relation and of an improved dispersion relation in comparison to calculations based on the dielectric function in random phase approximation is investigated. More important, this well-established treatment of Thomson scattering on free electrons is generalized in the Born-Mermin approximation by including collisions. We show that, in the transition region from collective to noncollective scattering, the consideration of collisions is important.

DOI: 10.1103/PhysRevE.78.026411 PACS number(s): 52.25.Os, 52.35.Fp, 71.45.Gm, 71.10.Ca

I. INTRODUCTION

A key issue in the diagnostics of dense plasmas is the determination of free electron density and temperature. Physical properties such as line profiles, bremsstrahlung spectrum, or Thomson scattering can be used for that purpose. In this context, knowledge of the plasmon resonance is necessary for the analysis of experimental data. Therefore, we discuss the applicability of the Gross-Bohm dispersion relation and options to go beyond it when considering the determination of plasma parameters in warm dense matter (WDM), where many-particle effects like collisions play an important role.

The region of WDM considered is relevant for, e.g., inertial confinement fusion experiments or models for planetary interiors. WDM is characterized by densities as typical for the solid state and temperatures of several eV. These plasmas are opaque in the optical region since the frequency of light, $\omega_0=2\pi c/\lambda_0$, is lower than the plasma frequency $\omega_{\mathrm{pe}}^2=n_e e^2/(\epsilon_0 m_e)$ of the free electron subsystem, with electron density n_e and electron mass m_e. Therefore, probing plasmas with densities approaching solids or even higher densities requires x-ray sources.

Powerful x-ray pulses are produced by energetic optical lasers [1] and then used to pump and probe samples in the near-solid density regime. The 4.75-keV titanium He-α backlighter [2,3] has been used to measure the noncollective Thomson scattering spectrum on solid density beryllium. From the shape of the Compton-shifted electron-scattering signal, the electron temperature could be detected. In another experiment, scattering from the collective electron plasma mode (plasmon) at solid density beryllium using a Cl Ly-α backlighter at 2.96 keV was performed [4].

Alternatively, the study of WDM will eventually be possible with new fourth-generation light sources [free electron lasers (FELs) in the vuv and x-ray regions] as a tool to probe near-solid density targets. Currently available is the FLASH facility at DESY, Hamburg, with wavelengths ranging from 7 to 50 nm in the vuv region [5,6]. The construction of an x-ray FEL is planned at DESY [7,8] in 2013. A similar project is currently under construction at the Stanford Linear Acceleration Center (SLAC) [9].

In plasmas at near-solid density, strong coupling effects are important. In particular, a consistent many-body theory is needed if the nonideality parameter Γ_e for electrons,

$$\Gamma_e = \frac{e^2}{4\pi\epsilon_0 k_{\mathrm{B}} T_e}\left(\frac{4\pi n_e}{3}\right)^{1/3}, \tag{1}$$

is larger than 1. The plasma parameters—i.e., the free electron temperature T_e and the free electron density n_e, as well as the ionization state Z—can be derived analyzing the Thomson-scattering signal. The electron temperature can be obtained using the method of detailed balance [4,10], while the electron density follows from the plasmon dispersion relation for collective scattering. In this paper, we discuss the measurement of the free electron density via the maximum position of the plasmon peak. We compare with the usual Gross-Bohm [11] dispersion relation $\omega_{\mathrm{GB}}(k)$. Furthermore, we analyze the improved dispersion relation (IDR) [10] accounting for higher-density effects, characterized by the degeneracy parameter Θ_e for electrons,

$$\Theta_e = \frac{2m_e k_{\mathrm{B}} T_e}{\hbar^2}(3\pi^2 n_e)^{-2/3}, \tag{2}$$

and higher orders of the scattering wave number. In Ref. [12], analytic results for the dynamic structure factor as the basic input for the Thomson-scattering cross section on the

*robert.thiele@uni-rostock.de

level of the random phase approximation (RPA) were shown. Recently, the influence of electron-ion collisions on the dynamic structure factor [13] was studied in addition. A systematic improvement of the Born approximation including dynamic screening, strong collisions, and electron-electron collisions by a renormalization factor of the collision frequency [14,15] has been accomplished by the use of thermodynamic Green's functions leading to the Gould-DeWitt [16] scheme. This can be extended to finite wave numbers k by the Mermin approach [17–19] in order to calculate the dynamic structure factor. In this way electron-ion collisions as well as electron-electron collisions have been accounted for in our approach.

For the interpretation and evaluation of state-of-the-art plasma experiments, accurate measurements of the Thomson-scattering signal are needed. Therefore, the scattering of photons on plasmas has been studied for a long time [20–24]. We will show that Thomson scattering can indeed serve as a reliable diagnostic tool to analyze plasma parameters such as, e.g., density, temperature, and plasma composition or to test the quality of the models used to determine the dynamic structure factor.

In the next section, we introduce the dynamic structure factor and the Born-Mermin approximation (BMA). In Sec. III, we study the position of the plasmon peak under the influence of collisions. The Gross-Bohm plasmon dispersion relation and the IDR are described in Sec. IV. The results for solid density plasmas are shown in Sec. V. We will conclude with a summary.

II. DYNAMIC STRUCTURE FACTOR

As described in [12,21,24,25], the Thomson-scattering cross section is related to the dynamic structure factor of all electrons in the plasma according to

$$\frac{d^2\sigma}{d\Omega\, d\omega} = \sigma_T \frac{k_1}{k_0} S_{ee}(k,\omega). \tag{3}$$

Here, $\sigma_T = 6.65 \times 10^{-29}\ \mathrm{m}^2$ is the Thomson cross section, k_0 and k_1 are the wave numbers of the incident and scattered light, and the energy and momentum transfers are given by $\Delta E = \hbar\omega = \hbar\omega_1 - \hbar\omega_0$ and $\hbar\mathbf{k} = \hbar\mathbf{k}_1 - \hbar\mathbf{k}_0$. The momentum is related to the scattering angle θ in the limit $\hbar\omega \ll \hbar\omega_0$ according to $k = 4\pi \sin(\theta_S/2)/\lambda_0$, with scattering angle θ_S and incident wavelength λ_0. Here, we follow Chihara's approach [21,24], in that the total dynamic structure factor can be written in terms of contributions from free electrons, weakly and tightly bound electrons, and core electrons. In the present paper, only the dynamic structure factor of free electrons is considered.

In thermodynamic equilibrium, the dynamic structure factor $S_{ee}(k,\omega)$ and the longitudinal dielectric function $\epsilon(k,\omega)$ are related via the fluctuation-dissipation theorem

$$S_{ee}(k,\omega) = -\frac{\epsilon_0 \hbar k^2}{\pi e^2 n_e} \frac{\mathrm{Im}\ \epsilon^{-1}(k,\omega)}{1 - \exp\left(-\dfrac{\hbar\omega}{k_B T_e}\right)}. \tag{4}$$

A peak in the dynamic structure factor or in the imaginary part of the inverse dielectric function,

$$\mathrm{Im}\ \epsilon^{-1}(k,\omega) = \frac{-\mathrm{Im}\ \epsilon(k,\omega)}{[\mathrm{Re}\ \epsilon(k,\omega)]^2 + [\mathrm{Im}\ \epsilon(k,\omega)]^2}, \tag{5}$$

can be interpreted as a resonant charge density excitation or plasmon. In general, the dielectric function is given in terms of the polarization function $\Pi(\vec{k},\omega)$ via

$$\epsilon(\vec{k},\omega) = 1 - \frac{1}{\epsilon_0 k^2}\Pi(\vec{k},\omega). \tag{6}$$

Neglecting collisions, the polarization function is given in the RPA as

$$\Pi^{\mathrm{RPA}}(\mathbf{k},\omega) = \frac{1}{\Omega_0}\sum_p e^2 \frac{f^e_{p+k/2} - f^e_{p-k/2}}{\Delta E^e_{p,k} - \hbar(\omega + \mathrm{i}\eta)}. \tag{7}$$

Here, Ω_0 is the normalization volume and $\Delta E^e_{p,k} = E^e_{p+k/2} - E^e_{p-k/2} = \hbar^2 \mathbf{k}\cdot\mathbf{p}/m_e$. Furthermore, $f^e_p = [\exp(E^e_p - \mu_e)/k_B T_e + 1]^{-1}$ denotes the Fermi distribution function and μ_e is the chemical potential of electrons. The limit $\eta \to 0$ has to be taken after the thermodynamic limit.

We improve the RPA by considering collisions and assume a Drude-like behavior for the damping of the frequency-dependent dielectric function via a collision frequency. Within linear response theory [19], the dynamic collision frequency $\nu(\omega)$ can be consistently introduced via the Mermin dielectric function

$$\epsilon^{\mathrm{M}}(k,\omega) - 1 = \frac{\left(1 + \mathrm{i}\dfrac{\nu(\omega)}{\omega}\right)[\epsilon^{\mathrm{RPA}}(k,\omega + \mathrm{i}\nu(\omega)) - 1]}{1 + \mathrm{i}\dfrac{\nu(\omega)}{\omega}\dfrac{\epsilon^{\mathrm{RPA}}(k,\omega + \mathrm{i}\nu(\omega)) - 1}{\epsilon^{\mathrm{RPA}}(k,0) - 1}}. \tag{8}$$

In [13,25], the influence of collisions on the dynamic structure factor was investigated for a wide range of temperatures and densities applying various approximations. In the so-called Born-Mermin approximation, we will evaluate the collision frequency in Born approximation with respect to a statically screened Debye potential which can be written [10,14,15] as

$$\nu^{\mathrm{Born}}(\omega) = -\mathrm{i}\frac{\epsilon_0 n_i \Omega_0^2}{6\pi^2 e^2 n_e m_e}\frac{1}{\omega}\int_0^\infty dq q^6 V_D^2(q) S_{ii}(q) \times [\epsilon^{\mathrm{RPA}}(q,\omega) - \epsilon^{\mathrm{RPA}}(q,0)], \tag{9}$$

with $S_{ii}(q)$ being the static ion-ion structure factor and $V_D(q) = -Ze^2/[\epsilon_0 \Omega_0 (q^2 + \kappa^2)]$ the statically screened electron-ion Debye potential. κ is the inverse screening length in the plasma, which is given for plasmas at any degeneracy by

$$\kappa^2 = \frac{e^2 m_e^{3/2}}{\sqrt{2}\pi^2 \epsilon_0 \hbar^3}\int_0^\infty dE_p E_p^{-1/2} f^e_p. \tag{10}$$

In the classical case, the well-known inverse Debye screening $\kappa_D^2 = n_e e^2/(\epsilon_0 k_B T_e)$ is obtained. The static ion-ion

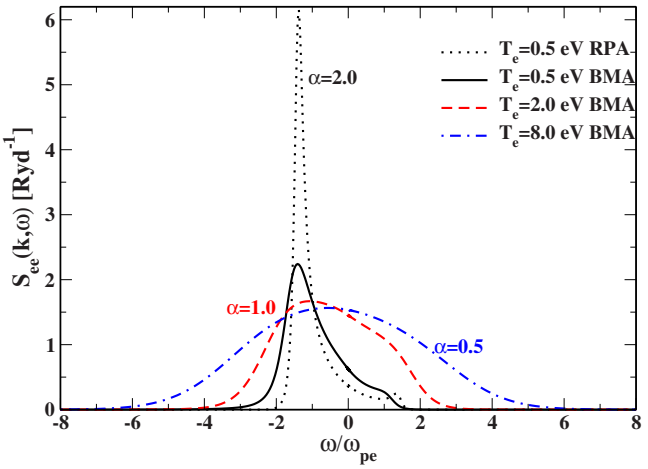

FIG. 1. (Color online) Electronic dynamic structure factor $S_{ee}(k,\omega)$ from collective (α=2.0) up to noncollective (α=0.5) Thomson scattering calculated in the RPA (black-dotted line) for T_e =0.5 eV and BMA (T_e=0.5, 2.0, 8.0 eV) for a fully ionized hydrogen plasma with $n_e=10^{21}$ cm^{-3}, a laser wavelength λ_0=4.13 nm, and a scattering angle θ_S=160°.

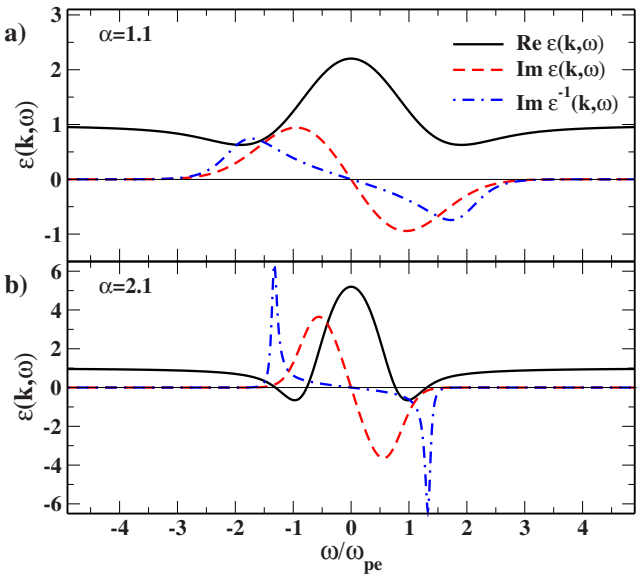

FIG. 2. (Color online) Dielectric function $\epsilon^{\mathrm{RPA}}(k,\omega)$ of electrons for electron densities: (a) $n_e=1.0\times10^{23}$ cm^{-3} (α=1.1) and (b) $n_e=5.0\times10^{23}$ cm^{-3} (α=2.1). The electron temperature is T_e =12 eV, laser wavelength λ_0=0.42 nm, and the scattering angle θ_S=40°.

structure factor $S_{ii}(q)$ accounts for ion correlations, which are particularly important in highly ionized materials. Here, we use S_{ii}=1 for an isotropic ion background. For improved expressions of $S_{ii}(q)$, see [26–28].

For applications to scattering experiments in WDM, the range of the wave number k of interest is given by the experimental setup. It allows us to discriminate between collective and noncollective scattering. Therefore, to further analyze the structure factor and Thomson scattering, the scattering parameter [29]

$$\alpha = \frac{\kappa}{k} \tag{11}$$

is introduced. For $\alpha<1$, the scattering is noncollective, and we can investigate short-range correlations within the Debye sphere [1]. Long-range correlations are relevant for collective scattering ($\alpha>1$). In this case, the electronic structure factor $S_{ee}(k,\omega)$ shows two particularly pronounced side maxima, found symmetrically to the central Rayleigh peak, which are related to the free electron density; see also [4]. In the following, we will restrict ourselves to the redshifted left peak since it is the one with the higher intensity.

In Fig. 1, the electronic dynamic structure factor $S_{ee}(k,\omega)$ in the RPA and BMA is shown for different conditions. For the lowest temperature (T=0.5 eV), we compare the RPA with the BMA calculations. The collisions broaden the structure factor and shift the left maximum of $S_{ee}(k,\omega)$ to higher frequencies. For higher temperatures, the differences between the RPA and BMA become smaller. Therefore, we show only the BMA calculations for the higher temperatures. More details of the influence of the collisions for a wide range of electron densities and temperatures are given in [13,25]. For collective scattering (α=2.0), we see a sharp peak near the electronic plasma frequency ω_{pe}. For noncollective scattering (α=0.5), only one maximum of $S_{ee}(k,\omega)$ is found and the peak is broadened due to thermal electronic motion. Within our approach, we now consider collective scattering with a scattering parameter $\alpha>1$. We will present results for the dielectric function in the Born-Mermin approximation, where the maximum position ω_{res} from $S_{ee}(k,\omega)$ is determined numerically as a function of density and temperature. Nevertheless, it is useful for plasma diagnostics to have analytical estimates for the peak position. We will aim at an improved plasmon dispersion relation below.

III. POSITION OF THE PLASMON PEAK IN THE DRUDE LIMIT

In the following, we will discuss the position of the maximum in the dynamic structure factor $S_{ee}(k,\omega)$ which is due to a redshift of the probing frequency and is related to the imaginary part of the inverse dielectric function according to Eq. (4). In the collective regime, the maximum position is the so-called plasmon peak or plasmon resonance. For strong collective scattering ($\alpha\gg1$), it is the long-wavelength limit ($k\to0$).

In Fig. 2, the real and imaginary parts of the dielectric function as well as the imaginary part of the inverse dielectric function, all calculated within the RPA via Eqs. (6) and (7), are shown for weakly collective (α=1.1) and collective (α=2.1) scattering. For α=2.1, the real part of the dielectric function has four zeros symmetrically positioned with respect to the plasma frequency. The plasmon peak of interest can be found at the zero of Re $\epsilon(k,\omega)$ with the highest absolute value of the frequency shift, because the imaginary part is minimal. Here, a narrow sharp peak of Im $\epsilon^{-1}(k,\omega)$ is obtained, typical for collective scattering. In the other case, for α=1.1, a zero of the real part of the dielectric function does not exist.

For an estimate of the influence of collisions, we discuss the position of the plasmon peak within the Drude model [30,31], obtained from the Mermin formula, Eq. (8), in the long-wavelength limit:

$$\lim_{k\to 0} \epsilon^{\mathrm{M}}(k,\omega) = \epsilon(\omega) = 1 - \frac{\omega_{\mathrm{pe}}^2}{\omega[\omega + i\nu(\omega)]}. \tag{12}$$

In the case of a static collision frequency $\nu=\nu(0)$ and Im $\nu=0$, the real and imaginary parts of the dielectric function are given by

$$\mathrm{Re}\ \epsilon(\omega) = \frac{\omega^2+\nu^2-\omega_{\mathrm{pe}}^2}{\omega^2+\nu^2}, \quad \mathrm{Im}\ \epsilon(\omega) = \frac{\nu}{\omega}\frac{\omega_{\mathrm{pe}}^2}{\omega^2+\nu^2}. \tag{13}$$

As a result, the imaginary part of the inverse dielectric function can be written in the following form:

$$\mathrm{Im}\ \epsilon^{-1}(\omega) = \frac{\nu\omega\omega_{\mathrm{pe}}^2(\omega^2+\nu^2)}{\omega^2(\omega^2+\nu^2-\omega_{\mathrm{pe}}^2)^2+\nu^2\omega_{\mathrm{pe}}^4}. \tag{14}$$

According to Eq. (4), the maximum position of $S_{ee}(k,\omega)$ can then be found at

$$\omega_{\mathrm{res}}^2 \approx \omega_{\mathrm{pe}}^2 - \frac{\nu^2}{4}, \tag{15}$$

assuming $\nu \ll \omega_{\mathrm{pe}}$. Thus, the plasmon peak is expected to shift due to collisions. In [25], the static collision frequency, normalized by the electronic plasma frequency, was shown for a wide range of free electron densities.

In contrast to Eq. (15), an estimate of the maximum position of $S_{ee}(k,\omega)$ from the dispersion relation Re $\epsilon(\omega)=0$, Eq. (13), leads to

$$\omega_0^2 = \omega_{\mathrm{pe}}^2 - \nu^2 = \omega_{\mathrm{pe}}^2\left(1 - \frac{\nu^2}{\omega_{\mathrm{pe}}^2}\right) = \omega_{\mathrm{pe}}^2\delta_\nu. \tag{16}$$

In Table I, we show the fraction ν/ω_{pe} and the deviation of the electronic plasma frequency δ_ν for the interesting range of electron densities and temperatures. It is found that $\nu \approx \omega_{\mathrm{pe}}$ only in the density region of $n_e=10^{21}$ cm^{-3} if typical temperatures for WDM are considered. Otherwise, $\nu \ll \omega_{\mathrm{pe}}$ [13] applies.

TABLE I. Static collision frequency in the Born approximation, normalized by the electronic plasma frequency for a wide range of the electron density-temperature plane. δ_ν describes the deviation of the electronic plasma frequency ω_{pe} via Eq. (16).

n_e (cm^{-3})	T_e (eV)	ν/ω_{pe}	δ_ν
10^{21}	0.5	0.654	0.573
	3.0	0.397	0.843
	12.0	0.101	0.990
10^{22}	0.5	0.098	0.990
	3.0	0.404	0.837
	12.0	0.183	0.967
10^{23}	2.0	0.082	0.993
	6.0	0.222	0.951
	12.0	0.215	0.954

In conclusion, the shift of the plasmon peak is a function of ν/ω_{pe} for both expressions. For $\nu \ll \omega_{\mathrm{pe}}$, the effect of collisions on the position of the plasmon peak can be neglected, as we will see later in the numerical results.

IV. PLASMON DISPERSION RELATION

Plasmons can be found as poles of $1/\epsilon(k,z)$ in the lower complex half plane (Im $z<0$) [32]. There are no general analytical results available, however. Assuming small Im $\epsilon(k,\omega)$, the peak is essentially determined by the solution of the dispersion relation

$$\mathrm{Re}\ \epsilon(k,\omega)\big|_{\omega=\omega_0(k)} = 0 \tag{17}$$

or, at least, by a minimum of Re $\epsilon(k,\omega)$. Considering the case of the RPA, we present plasmon dispersion relations in different approximations.

Starting from the Lindhard formula [see Eq. (7)], the real part of the dielectric function can be written as [33]

$$\mathrm{Re}\ \epsilon(k,\omega) = 1 - \frac{\omega_{\mathrm{pe}}^2}{\omega^2} \times \left[1 + \frac{z^2}{u^2} + \frac{3}{2}\frac{F_{3/2}(\eta)}{u^2 D^{5/2}} + \frac{3}{2}\frac{F_{5/2}(\eta)}{u^4 D^{7/2}} + \cdots\right] \tag{18}$$

for $z \ll u$, with $u=\omega/kv_F$, $z=k/2k_F$, $\eta=\mu_e/k_BT_e$, and $D=1/\Theta_e$. The velocity v_F corresponds to the Fermi wave number $k_F=m_e v_F/\hbar=(3\pi^2 n_e)^{1/3}$. The Fermi integrals $F_j(x)$ are defined by Eq. (A3). From $z \ll u$, the condition $k^2 \ll 2m_e\omega/\hbar$ is derived. Since we are interested in the behavior at ω_{pe}, this limits the applicability of Eq. (18) to the wave number k

$$k^2 \ll \frac{2m_e}{\hbar}\sqrt{\frac{e^2 n_e}{\epsilon_0 m_e}}. \tag{19}$$

From this, a minimum density $n_{\mathrm{min}}=\hbar^2k^4\epsilon_0/(4m_e e^2)$ follows for an experimental setup with given wave number k. Assuming the approximation (18), the dispersion relation (17) for the RPA is solved by

$$\omega_0^2(k) = \omega_{\mathrm{pe}}^2\left[1 + \frac{\langle p^2\rangle}{m_e^2}\frac{k^2}{\omega_0^2(k)} + \left(\frac{\hbar}{2m_e}\right)^2\frac{k^4}{\omega_0^2(k)} + \frac{\langle p^4\rangle}{m_e^4}\frac{k^4}{\omega_0^4(k)} + \cdots\right], \tag{20}$$

with the moments $\langle p^i \rangle$ related to the Fermi integrals defined by Eq. (A1).

In the classical limit ($\Theta \gg 1$), $\langle p^2 \rangle = 3k_B T_e m_e$, and by neglecting terms beyond the order of k^2, we obtain the well-known Gross-Bohm dispersion relation [11]

$$\omega_{\mathrm{GB}}^2(k) = \omega_{\mathrm{pe}}^2 + \frac{3k_B T_e}{m_e} k^2. \tag{21}$$

The plasmon resonance ω_{GB} in the Gross-Bohm relation is approximated by the electron plasma frequency ω_{pe} and an additional term which depends on electron temperature and scattering wave number only.

For a weakly degenerate electron gas with $\Theta \approx 1$, the Fermi integrals can be expanded [see Eq. (A4)]. Considering quantum diffraction and the third term in Eq. (20), we derive the IDR

$$\omega_{\mathrm{IDR}}^2 = \omega_{\mathrm{pe}}^2 + \frac{3k_B T_e}{m_e} k^2 (1 + 0.088 n_e \Lambda_e^3) + \left(\frac{\hbar k^2}{2m_e} \right)^2. \tag{22}$$

The last term in Eq. (20) is in order of k^4 and ω^{-4}. This effect can be neglected for the densities and wave numbers investigated. In comparison to the Gross-Bohm dispersion relation, the range of applicability is extended to higher wave numbers (larger scattering angles) and higher densities (or lower temperatures).

V. RESULTS FOR WDM

We will now compare the position of the maximum $\Delta E = \hbar \omega_{res}$ of the dynamic structure factor $S_{ee}(k, \omega)$ in BMA [see Eqs. (4)–(9)], with the well-known Gross-Bohm dispersion relation $\omega_{\mathrm{GB}}(k)$, Eq. (21), for typical FLASH wavelengths $\lambda_0 = (32.0, 13.5, 6.0)$ nm.

First, we calculate these quantities for a fully ionized hydrogen plasma in the electron density range $n_e = (10^{21} - 10^{24})$ cm^{-3} with two different electron temperatures $T_e = 1$ eV and $T_e = 20$ eV (see Fig. 3). These conditions are relevant for collective Thomson-scattering experiments at FLASH [10]. The scattering setup with the laser wavelength λ_0 and the scattering angle θ_S was chosen for a wide range of wave numbers k available at FLASH. For the highest wavelength $\lambda_0 = 32$ nm, the differences between the Gross-Bohm relation and the BMA are very small. The second term in Eq. (21) can be neglected, because the wave number is small. For these conditions, the maximum position of $S_{ee}(k, \omega)$ can be found at the electron plasma frequency ω_{pe}, and it is independent of the electron temperature T_e. The limit of the density n_{min} is orders of magnitude smaller than the lowest density $n_e = 10^{21}$ cm^{-3} (see Table II).

In the intermediate-wavelength region ($\lambda_0 = 13.5$ nm), small differences occur between $T_e = 1$ eV and $T_e = 20$ eV for smaller densities (see Fig. 3). The wave number increases, and the temperature dependence due to the second term in Eq. (21) becomes important. The Gross-Bohm dispersion relation is valid; the limiting density n_{min} is still orders of magnitude smaller than the densities investigated.

For the lowest wavelength $\lambda_0 = 6$ nm, the temperature dependence of the energy shift is pronounced for a wide density range. The second term in Eq. (21) becomes more important. Furthermore, the Gross-Bohm dispersion relation differs strongly from the BMA for $T_e = 20$ eV in the lower-density range $n_e = 10^{21} - 10^{22}$ cm^{-3}. Here, the limit of applicability of the dispersion relation (20) is clearly visible.

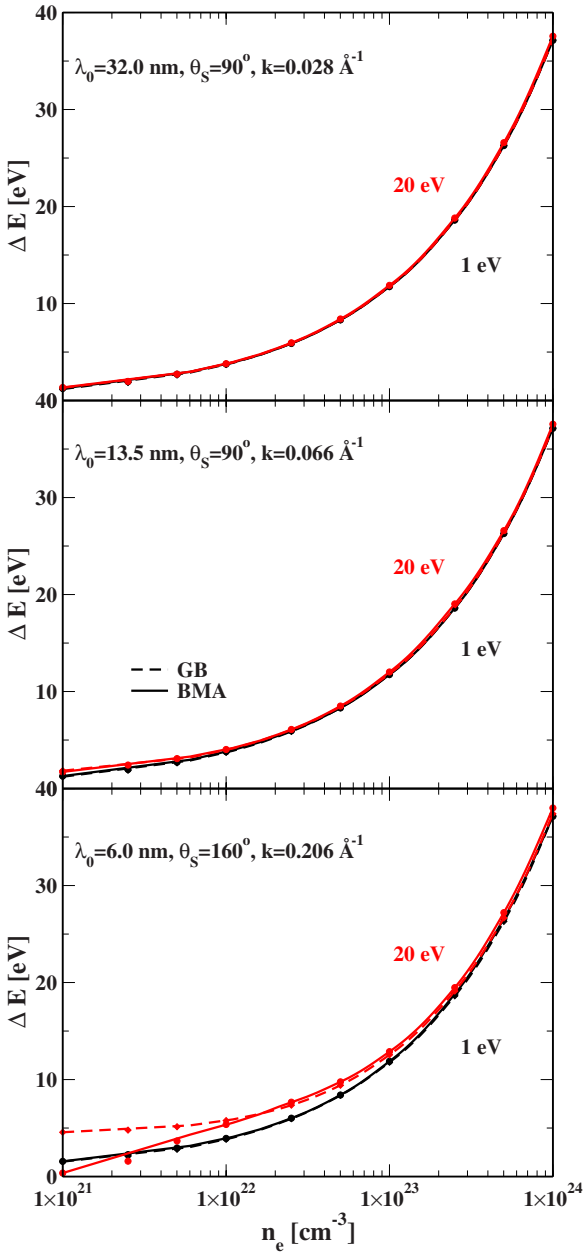

FIG. 3. (Color online) Comparison of the maximum position ΔE of $S_{ee}(k, \omega)$ in the BMA (solid lines) with the energy shift $\omega_{\mathrm{GB}}(k)$ (dashed lines) as a function of the electron density n_e for a fully ionized hydrogen plasma at electron temperatures $T_e = 1$ eV (black lines) and $T_e = 20$ eV (red lines). The scattering setup for the different wave numbers k is given in Table II.

We have shown that for the wavelengths available at FLASH, the Gross-Bohm dispersion relation yields good results for the determination of the free electron density via the energy shift of the Thomson-scattering signal. The temperature becomes important at lower densities; the resonance frequency can be found near the electron plasma frequency.

TABLE II. Exemplary experimental setup with the laser wavelength λ_0, the scattering angle θ_S, and the corresponding wave number k. The density $n_{\min}$ describes the lower limit of the electron density for the validity of the Gross-Bohm dispersion relation.

λ_0 (nm)	θ_S	k (Å^{-1})	$n_{\min}$ (cm^{-3})
32.0	90°	0.028	1×10^{16}
13.5	90°	0.066	3×10^{17}
6.0	160°	0.206	2×10^{19}
0.42	40°	1.020	1×10^{22}

With increasing wave number k or decreasing wavelengths, the differences between the Gross-Bohm relation and the BMA become larger.

Now, we will study the applicability of the dispersion relation for x-ray Thomson scattering. A beryllium plasma has been produced and investigated in pump-probe experiments at the Omega laser facility [4,34] with wavelength $\lambda_0=0.42$ nm in the x-ray region. Electron temperatures of $T_e=12$ eV were obtained and the scattering signal was observed for different angles and wave numbers.

Figure 4 shows the energy shift of the maximum of the Thomson-scattering signal for different free electron densities depending on wave number k and scattering angle θ_S. The wave numbers are more than 5 times larger than in the FLASH region (see also Table II). For these wave numbers and for the plasma parameters of interest, the IDR has to be used instead of the Gross-Bohm dispersion relation, because the second term in Eq. (20) becomes important. The scattering parameter α decreases with increasing wave number or scattering angle and decreasing electron density. For $n_e=1.0\times10^{23}$ cm^{-3}, the scattering parameter varies from $\alpha=1.5$ to $\alpha=0.5$ for given scattering angles $\theta_S=30°-90°$, respectively. Obviously, for higher wave numbers and angles, the limit of applicability of the IDR is reached where the IDR crosses the BMA. Therefore, the differences between the IDR and BMA are significant for higher wave numbers and towards lower densities. Furthermore, for $\theta_S>40°$, the scattering is noncollective. In this region, the BMA is superior to the RPA; there are slight differences between the BMA and RPA.

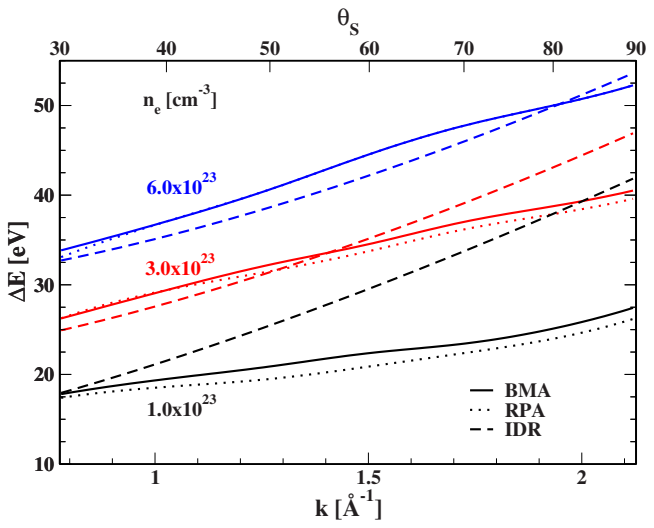

FIG. 4. (Color online) Comparison of the maximum position ΔE of $S_{ee}(k,\omega)$ in the RPA (dotted line) and BMA (solid line) with the energy shift of the IDR (dashed line) in dependence on wave number k and scattering angle θ_S, respectively, for Thomson scattering on beryllium plasma with $Z_{\text{eff}}=2.5$, $n_e=(1.0,3.0,6.0)\times10^{23}$ cm^{-3}, $T_e=12$ eV, and laser wavelength $\lambda_0=0.42$ nm.

It would be very helpful for an evaluation of experiments to derive a fit formula for the BMA calculations of the maximum position ΔE (in eV) as a function of the electron density n_e at a given temperature T. Here, we give an example for the wave number $k=1.02$ Å^{-1} corresponding to $\lambda_0=0.42$ nm in Table II. Fit parameters for other wave numbers are available upon request. Defining a decadic logarithm of the density $x=\log_{10}(n_e/n_0)$ with a reference density of $n_0=10^{20}$ cm^{-3}, the maximum position is obtained from

$$\Delta E = a_0 + a_1 x + a_2 x^2 + a_3 x^3 + a_4 \sqrt{x}. \tag{23}$$

The temperature-dependent coefficients are given by

$$a_0(T) = 223.3 - 23.8T,$$

$$a_1(T) = 344.0 - 37.7T,$$

$$a_2(T) = -55.9 - 6.00T,$$

$$a_3(T) = 5.64 - 0.52T,$$

$$a_4(T) = -512.7 + 56.0T,$$

with T in eV. The fit reproduces the BMA maximum position within an accuracy of 1% for temperatures between 1 eV and 20 eV and densities between 10^{21} cm^{-3} and 10^{24} cm^{-3}.

Next, we study the applicability of the Gross-Bohm (GB) relation and IDR for a given Thomson-scattering experiment [4] in the solid density region and for x-ray wavelengths. In Fig. 5, the dependence of the maximum position of $S_{ee}(k,\omega)$ in the RPA and BMA on the free electron density is shown, together with the energy shift in the IDR and Gross-Bohm relation and the zeros of the real part of the dielectric function in the RPA. In addition, we compare with results following from the dielectric function which was calculated including local field corrections (LFCs) [35] and an experimental point taken from [4]. In the considered density range, the differences between the structure factor calculations and the dispersion relations are considerable. For densities smaller than $n_e=2.8\times10^{23}$ cm^{-3}, the scattering parameter α is lower than 1, and zeros of Re $\epsilon(k,\omega)$ do not exist. Again, the GB relation and IDR are not applicable. The shift of the maximum position obtained from the BMA is smaller compared to the RPA due to the relevance of collisions in this region.

For higher densities ($n_e\geqslant4.0\times10^{23}$ cm^{-3}), the maximum position is not affected by collisions. The BMA and RPA give the same result. For the strongly collective regime, the zeros of the real part of the dielectric function can be found at the same energy as the maximum position of $S_{ee}(k,\omega)$. For the highest densities and collective scattering, the difference between the Gross-Bohm dispersion relation and BMA is

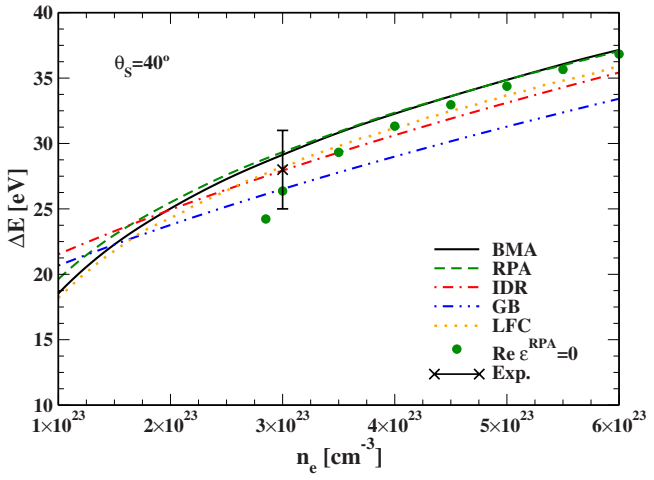

FIG. 5. (Color online) Comparison of the maximum position ΔE of $S_{ee}(k,\omega)$ in the RPA (green-dashed line) and BMA (black-solid line) with the energy shift in the GB dispersion relation (blue dash-dotted line) and IDR (red dash-dotted line) and local field corrections (LFC: orange dotted line) [35] in dependence on electron density n_e for a beryllium plasma with $Z_{\mathrm{eff}}=2.5$, $T_e=12$ eV, and laser wavelength $\lambda_0=0.42$ nm and scattering angle $\theta_S=40°$. The green points are the zeros of Re $\epsilon(k,\omega)$, and the experimental point is taken from [4].

approximately 4 eV. The improved dispersion relation with respect to quantum effects underestimates the energy shift by about 2 eV. These differences are significant; a few eV shift leads to an error of more than 30% in the free electron density.

VI. SUMMARY

We have discussed the plasmon resonance position of the dynamic structure factor $S_{ee}(k,\omega)$, the usual Gross-Bohm dispersion relation, and an improved dispersion relation. This is relevant for the determination of the free electron density in WDM. We have calculated the energy shift observed for the FLASH wavelength region. The differences between the Gross-Bohm dispersion relation and the maximum position of the dynamic structure factor in the BMA are small. The BMA is only needed for the determination of the free electron density with wavelengths near $\lambda_0=6$ nm and lower densities. For solid targets probed by x rays, the density should be calculated from the maximum position of $S_{ee}(k,\omega)$ in the BMA. In this region, simple dispersion relations (GB and IDR) are not applicable.

We conclude that collision effects are important [13] in WDM and can be considered within the BMA. A reliable density determination can only be done by numerically solving the BMA and inspecting the poles of Im $\epsilon^{-1}(k,\omega)$. A simple analytical fit formula for the position of the plasmon can be given for any laser wavelength.

ACKNOWLEDGMENTS

This work was supported by the virtual institute VH-VI-104 of the Helmholtz association and the Sonderforschungsbereich SFB 652. The work by S.H.G. was performed under the auspices of the U.S. Department of Energy by Lawrence Livermore National Laboratory under Contract No. DE-AC52-07NA27344. S.H.G. was also supported by LDRDs 08-ERI-002; 08-LW-004, and the Alexander von Humboldt Foundation. The work of G.G. was partially supported by the Science and Technology Facilities Council of the United Kingdom.

APPENDIX

We discuss the calculation of Eq. (20). The prefactors $\langle p^i\rangle$ are defined as [33]

$$\langle p^i\rangle = \frac{2}{n_e}\int \frac{d^3p}{(2\pi)^3} p^i f_e(p). \tag{A1}$$

The prefactor $\langle p^2\rangle$ of the k^2 term in Eq. (20) is proportional to the mean energy of the (ideal) Fermi system and allows one, therefore, to incorporate quantum statistical corrections. Especially, we have

$$\langle p^2\rangle = \frac{3}{2}k_B T_e \frac{1}{y} F_{3/2}(x), \tag{A2}$$

with the parameter $y=n_e\Lambda_e^3/2$, the thermal wavelength $\Lambda_e = h/\sqrt{2\pi m_e k_B T_e}$, $x=\beta\mu$, and the Fermi integrals

$$F_j(x) = \frac{1}{\Gamma(j+1)}\int_0^\infty \frac{t^j\, dt}{e^{t-x}+1}. \tag{A3}$$

In order to supply the reader with tractable expressions [36,37], we give the following result:

$$F_{3/2}(y)=\begin{cases} y+0.1768y^2-0.0033y^3+0.000094y^4, & y<5.5, \\ 0.4836y^{5/3}+1.3606y^{1/3}-1.7y^{-1}, & y>5.5. \end{cases} \tag{A4}$$

The parameter y can be estimated from $y=0.1656(n_e/10^{21}\ \mathrm{cm}^{-3})/(k_B T_e/\mathrm{eV})^{3/2}$. For the conditions of solid density beryllium [4], $y\leqslant 2$, one can use $1/yF_{3/2}(y)=1+0.1768y$ with an accuracy of better than 1%. With Eq. (A4), Eq. (20) can be solved to the order of k^4, and we get Eq. (22).

[1] O. L. Landen, S. H. Glenzer, M. J. Edwards, R. W. Lee, G. W. Collins, R. C. Cauble, W. W. Hsing, and B. A. Hammel, J. Quant. Spectrosc. Radiat. Transf. **71**, 465 (2001).
[2] S. H. Glenzer, G. Gregori, R. W. Lee, F. J. Rogers, S. W. Pollaine, and O. L. Landen, Phys. Rev. Lett. **90**, 175002 (2003).
[3] S. H. Glenzer, G. Gregori, F. J. Rogers, D. H. Froula, S. W. Pollaine, R. S. Wallace, and O. L. Landen, Phys. Plasmas **10**, 2433 (2003).
[4] S. H. Glenzer, O. L. Landen, P. Neumayer, R. W. Lee, K. Widmann, S. W. Pollaine, R. J. Wallace, G. Gregori, A. Höll, T. Bornath *et al.*, Phys. Rev. Lett. **98**, 065002 (2007).
[5] A. Kondratenko and E. Saldin, Part. Accel. **10**, 207 (1980).
[6] R. Bonifacio, C. Pellegrini, and L. Narducci, Opt. Commun. **50**, 373 (1984).
[7] *TESLA—Technical Design Report Part V: The X-Ray Free Electron Laser*, edited by G. Materlik and T. Tschentscher (DESY, Hamburg, 2001).
[8] *TESLA XFEL Technical Design Report (Supplement)*, edited by R. Brinkmann, K. F. B. Faatz, J. Rossbach, J. R. Schneider, H. Schulte-Schrepping, D. Trines, T. Tschentscher, and H. Weise (DESY, Hamburg, 2002).
[9] *LCLS Design Study Report* (The LCLS Design Study Group, SLAC, Stanford, CA, 1998).
[10] A. Höll, T. Bornath, L. Cao, T. Döppner, S. Düsterer, E. Förster, C. Fortmann, S. H. Glenzer, G. Gregori, T. Laarmann *et al.*, High Energy Density Phys. **3**, 120 (2007).
[11] D. Bohm and E. P. Gross, Phys. Rev. **75**, 1851 (1949).
[12] G. Gregori, S. H. Glenzer, W. Rozmus, R. W. Lee, and O. L. Landen, Phys. Rev. E **67**, 026412 (2003).
[13] A. Höll, R. Redmer, G. Röpke, and H. Reinholz, Eur. Phys. J. D **29**, 159 (2004).
[14] H. Reinholz, R. Redmer, G. Röpke, and A. Wierling, Phys. Rev. E **62**, 5648 (2000).
[15] R. Thiele, R. Redmer, H. Reinholz, and G. Röpke, J. Phys. A **39**, 4365 (2006).
[16] H. A. Gould and H. E. DeWitt, Phys. Rev. **155**, 68 (1967).
[17] N. D. Mermin, Phys. Rev. B **1**, 2362 (1970).
[18] G. Röpke, A. Selchow, A. Wierling, and H. Reinholz, Phys. Lett. A **260**, 365 (1999).
[19] A. Selchow, G. Röpke, A. Wierling, H. Reinholz, T. Pschiwul, and G. Zwicknagel, Phys. Rev. E **64**, 056410 (2001).
[20] D. E. Evans and J. Katzenstein, Rep. Prog. Phys. **32**, 207 (1969).
[21] J. Chihara, J. Phys. F: Met. Phys. **17**, 295 (1987).
[22] V. N. Tsytovich, Astropart. Phys. **5**, 285 (1996).
[23] E. Nardi, Z. Zinamon, D. Riley, and N. C. Woolsey, Phys. Rev. E **57**, 4693 (1998).
[24] J. Chihara, J. Phys.: Condens. Matter **12**, 231 (2000).
[25] R. Redmer, H. Reinholz, G. Röpke, R. Thiele, and A. Höll, IEEE Trans. Plasma Sci. **33**, 77 (2005).
[26] V. Schwarz, T. Bornath, W. D. Kraeft, S. Glenzer, A. Höll, and R. Redmer, Contrib. Plasma Phys. **47**, 324 (2006).
[27] K. Wünsch, P. Hilse, M. Schlanges, and D. O. Gericke, Phys. Rev. E **77**, 056404 (2008).
[28] D. Semkat, R. Redmer, and T. Bornath, Phys. Rev. E **73**, 066406 (2006).
[29] E. E. Salpeter, Phys. Rev. **120**, 1528 (1960).
[30] P. Drude, Ann. Phys. **39**, 504 (1890).
[31] A. Selchow, G. Röpke, and A. Wierling, Contrib. Plasma Phys. **42**, 43 (2002).
[32] W. Kraeft, D. Kremp, W. Ebeling, and G. Röpke, *Quantum Statistics of Charged Particle Systems* (Akademie-Verlag, Berlin, 1986).
[33] N. R. Arista and W. Brandt, Phys. Rev. A **29**, 1471 (1984).
[34] J. M. Soures, R. L. McCrory, C. P. Verdon, A. Babushkin, R. E. Bahr, T. R. Boehly, R. Boni, D. K. Bradley, D. L. Brown, R. S. Craxton *et al.*, Phys. Plasmas **3**, 2108 (1996).
[35] G. Gregori, A. Ravasio, A. Höll, S. Glenzer, and S. Rose, High Energy Density Phys. **3**, 99 (2007).
[36] H. M. Antia, Astrophys. J., Suppl. Ser. **84**, 101 (1993).
[37] R. Zimmermann, *Many-Particle Theory of Highly Excited Semiconductors* (Teubner-Verlag, Leipzig, 1988).